Received December 28, 2019, accepted February 21, 2020, date of publication February 27, 2020, date of current version March 10, 2020.

Digital Object Identifier 10.1109/ACCESS.2020.2976520

Radiation Measurement and Analysis of Power Line Communication System for Power Meter Reading

WENJUN PENG, WEIDONG ZHANG, AND BO AN

State Key Laboratory of Alternate Electrical Power System With Renewable Energy Sources, North China Electric Power University, Beijing 102206, China

Corresponding author: Wenjun Peng (peng_w_j@163.com)

ABSTRACT This paper is to study the effect of power line communication (PLC) system for power meter reading on electromagnetic environment. The experimental system of PLC for testing radiated disturbance is set up. The testing methods match the regulation of FCC Part 15. The simulation model of PLC is established using method of moment, and its effectiveness is verified by comparing the calculated results with the measured data. At application sites of power meter reading, the voltage at the beginning of the power lines and the radiated intensity at typical measurement points in the area are measured under three operating conditions of PLC system. Data reveal that the voltages are different under three operating conditions, which indicates that the impact brought by PLC operation is obvious. For the straight power lines, longitudinal distribution of radiation is fluctuant, and lateral attenuation of radiation is significant and rapid with a perceived range of 100-150 m. For crossed power lines, radiated distribution fluctuates remarkably. We can effectively predict the radiated distribution trend of PLC using simulation models. Moreover, multiple tests have shown that the radiated intensity in the application field is relatively high, because the environmental background noise plays a particularly large role. Comparing the operation and shutdown of the PLC system, the radiated contribution value can reach 15 dB at a lateral measuring distance of 10 m. Furthermore, we propose some recommendations for measurement methods.

INDEX TERMS Electromagnetic environment, electromagnetic measurement, method of moment (MOM), power line communication (PLC), radiated distribution.

I. INTRODUCTION

Power Line Communication (PLC) is a technology for transmitting data and media signals through existing power lines [1]. With the extensive coverage of the power networks, the advantage of PLC is that it does not need to specially set up and maintain dedicated communication lines, which greatly reduces deployment costs and easily be accepted. Moreover, modern PLC can have a high data rates [2] and thus applied to smart grids and indoor networking [1], [3]. Compared with the inefficient wireless transmission affected by the occlusion and reflection of dense buildings, power meter reading based on PLC technology has been popularized in China. Additionally, as State Grid Corporation of China proposed to build the ubiquitous power internet of things in January 2019, PLC, as one of the technologies, will have further development in the future.

Power networks are designed to reduce energy loss and deliver power reliably, not to transmit high-speed data. For efficient communications through power lines, numerous practical challenges must be overcome such as noise, multipath, interference, attenuation and electromagnetic interference (EMI) [4], [5]. To date, scholars have carried out some research to overcome aforementioned challenges. Carrier modulation technology and relaying protocol are two effective strategies [6], [7]. Researches on the relay selection problem, energy efficiency issues and performance of PLC systems are also abundant [7]–[11]. In addition, other special studies of PLC are carried out. The analysis and modeling of the power line channel are relatively complete, which is in good agreement with actual measurement and has wide applicability [12]–[14]. The authors in [15]–[17] discussed certain noise disturbances in PLC systems and

The associate editor coordinating the review of this manuscript and approving it for publication was Mehmet Alper Uslu.

This work is licensed under a Creative Commons Attribution 4.0 License. For more information, see http://creativecommons.org/licenses/by/4.0/

proposed effective solutions. Moreover, the electromagnetic compatibility (EMC) issues has been another key point in the development and application of PLC. The principle of radiated EMI and methods to suppress the EMI in PLC networks were studied [18], [19]. Limits of radiated disturbance in international standards are often given in the form of electric field strength, such as FCC PART15 in the United States, NB30 in Germany [20]. These international standards are currently only used as preliminary guidelines and PLC standards are still under discussion.

Despite many researches done on various technical aspect of PLC, the content of radiated disturbance measurement and analysis for PLC systems is still lacking. The radiated disturbance induced by existing systems in the environment may affect the normal operation of PLC system. On the other hand, little research has been done on the radiated distribution characteristics of field PLC. And field measurement methods of radiated disturbance and PLC standards have not yet determined internationally. What's more, in China, some regulatory authorities doubt the influence on electromagnetic environment after the deployment of PLCs, and need the industry clarification. All these indicate that the research on the radiated disturbance of the PLC system needs to be done urgently. Different from traditional narrowband PLC, broadband PLC technology for power meter reading widely used in China makes remote meter reading more efficient and convenient. In this paper, the radiation of broadband PLC is studied. The experimental system of PLC is set up, and we measure the radiated intensity at typical measurement points in the area. The PLC simulation model is established using the moment method (MoM), and the validity of the model is verified. We carry out a large number of field measurement work at the application site of power meter reading to obtain the operating voltage and radiated intensity of PLC. The radiated intensity is evaluated, and the radiated distribution trend can be predicted by simulation modeling. The main contribution of this paper resides in analyzing the practical radiated distribution characteristics of PLC with measured and calculated data and putting forward a series of recommendations for measurement methods, which has reference value for the development of PLC standards.

II. EXPERIMENTAL TESTING AND ANALYSIS

A. EXPERIMENTAL TESTING

To reduce the influence of the environment on the measurement results, the testing is performed in an open area. Two stacked horizontal power lines with a length of 100 m and a nominal cross-sectional area of 2.5 mm^2 are arranged above ground. The heights of two wires are 4.2 m and 3.4 m, respectively. At the beginning of the lines (defined as the position of 0 m), the primary side of a small isolation transformer (IT) is connected with 220V/50Hz ac power, and the secondary side supplies power to a DJGZ23-XLJ101 concentrator (EUT) through magnetic rings, which is to isolate possible interference from the power networks. At the terminal of the line (defined as the position of 100 m), a meter is connected. The working bandwidth of the whole experimental system is concentrated in the frequency range of 2.441-5.615 MHz. An antenna and a handheld spectrum analyzer are used as measuring equipment. The parameter settings of the spectrum analyzer are shown in Table 1. Considering the variation of the working spectrum of PLC system, the radiated intensity measured is based on measuring equipment employing peak detector function and Maxhold function. The Maxhold function refers to multiple sweeps and retaining the maximum value at each frequency eventually, which ensures that the strongest radiation is captured during the measurement period. This is very representative for assessing the severity of PLC radiation.

According to FCC Part15, if the mid-band frequency used by the EUT does not exceed the lowest frequency injected onto the power line by more than a factor of two, testing should be performed at distances of 0, 1/4, 1/2, 3/4, and 1 wavelength of the mid-band frequency from the PLC injection point on the power line. Thus we choose five measurement points as shown in Fig. 1. The lateral distance (D_L) between the measurement point and the power line is 10 m. The complete experimental system is shown in Fig. 2.

TABLE 1. Parameters of N9344C spectrum analyzer.

Parameter	Description
frequency	2 MHz - 6 MHz
detector	PK
bandwidth	10 kHz
measurement mode	sweep
trace	Maxhold

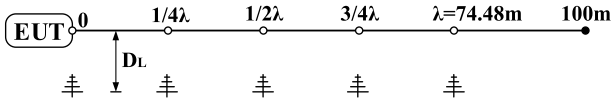

FIGURE 1. Measurement points position.

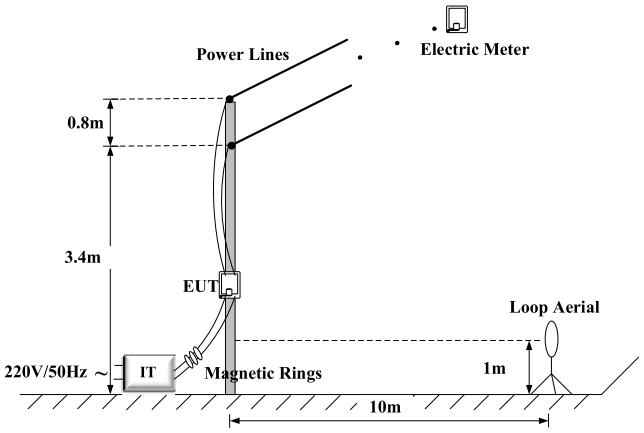

FIGURE 2. Experimental system.

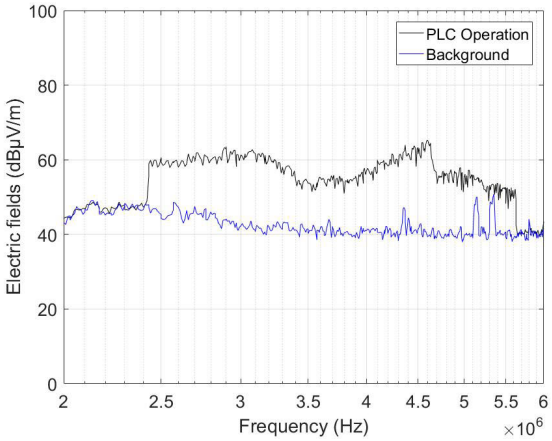

(a)

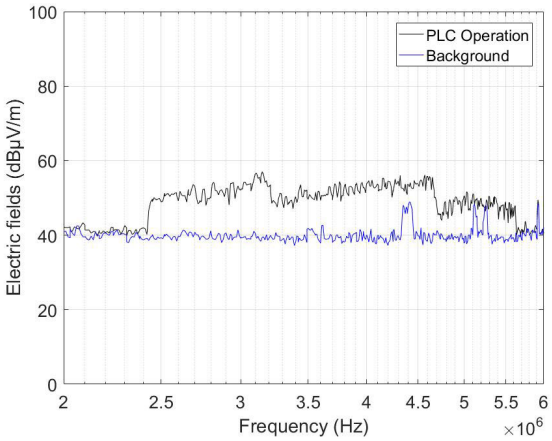

(b)

FIGURE 3. Measured radiated intensity of PLC operation and background noise: (a) measurement point 1/4λ and (b) measurement point λ.

Under the aforementioned testing conditions, we obtain the data. From Fig. 3, we can see that the electric field intensity measured when the PLC system is operating is significantly higher than the background noise measured when the PLC system is turned off in the frequency range of 2.441-5.615 MHz. This indicates that the radiation measured has a certain causal relationship with the work of the PLC system.

Although the radiated disturbance intensity generated by PLC can be tested through experimental system or at application sites, this alone is not sufficient to study its spatial distribution characteristics. Therefore, the simulation model of PLC is to establish using suitable mathematic method.

B. CALCULATION METHOD

The radiated disturbance is mainly caused by high-frequency signals carried in power line, which is like an antenna. And it belongs to the category of electrically large. The method of moment (MOM) only needs to discrete geometrical model

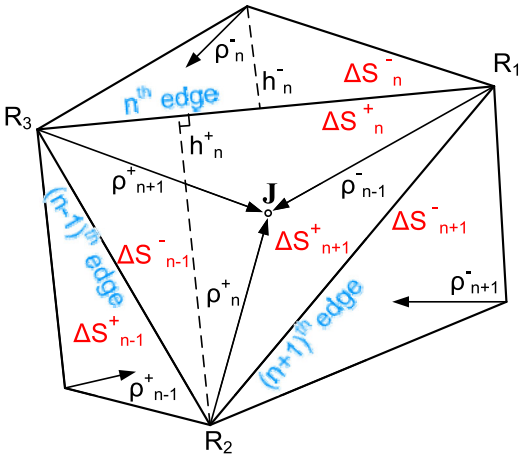

FIGURE 4. Triangulation for scattered metal.

without space, and there is no need to set boundary conditions. Its computational complexity only depends on the calculated frequency and the geometric size of the model. Therefore, the MOM is selected to calculate the radiated disturbance of PLC in this paper.

The Maxwell equations in the passive region of free space is

$$\nabla \times \mathbf{E} = -j\omega\mu\mathbf{H} \tag{1}$$

$$\nabla \times \mathbf{H} = j\omega\varepsilon\mathbf{E} \tag{2}$$

Electric field can be computed by [21]

$$\mathbf{E}_S = -\nabla\Phi - j\omega\mathbf{A} \tag{3}$$

with the scalar potential defined as

$$\Phi\left(\mathbf{r}, \mathbf{r}'\right) = -\frac{1}{4\pi\varepsilon j\omega}\int_S \nabla\cdot\mathbf{J}\frac{e^{-jkR}}{R}dS \tag{4}$$

and the magnetic vector potential as

$$\mathbf{A}\left(\mathbf{r}, \mathbf{r}'\right) = \frac{\mu}{4\pi}\int_S \mathbf{J}\frac{e^{-jkR}}{R}dS \tag{5}$$

where $R = \left|\mathbf{r} - \mathbf{r}'\right|$ is the distance between an observation point $\mathbf{r}$ and a source point $\mathbf{r}'$, $\mathbf{J}$ is the surface current and $k = \omega\sqrt{\mu\varepsilon} = 2\pi/\lambda$ is the wave number. Hence, (3) can be written as

$$\mathbf{E}_S = \frac{\nabla}{4\pi\varepsilon j\omega}\int_S \nabla\cdot\mathbf{J}\left(\mathbf{r}'\right)\frac{e^{-jkR}}{R}dS - \frac{j\omega\mu}{4\pi}\int_S \mathbf{J}\left(\mathbf{r}'\right)\frac{e^{-jkR}}{R}dS \tag{6}$$

A suitable triangulation has been found to scattered metal, as shown in Fig. 4. One can also see that each edge (for example edge n) corresponds to two different triangles (for example triangles ΔS_n^+ and ΔS_n^-). The sign "+" or "−" indicates that the triangle of the calculated observation point is marked as "+" or "−" for nth edge. $h_n^\pm$ is the height of triangle $\Delta S_n^\pm$ with edge n as the base. $\boldsymbol{\rho}_n^\pm$ is the vector pointing from the vertex, opposite nth edge, to some point in the triangle. $\mathbf{J}$ at any source point $\mathbf{r}'$ in the triangle can

be composed by three vectors pointing from that point to the three vertices, which can be expressed as follows

$$\mathbf{J}\left(\mathbf{r}'\right) = \sum_{n=1}^{3} J_n \mathbf{f}_n \tag{7}$$

with basis function $\mathbf{f}_n$ expressed as

$$\mathbf{f}_n = \begin{cases} -\dfrac{\boldsymbol{\rho}_n^-}{h_n^-}, & \boldsymbol{\rho}_n^- \in \Delta S_n^- \\ +\dfrac{\boldsymbol{\rho}_n^+}{h_n^+}, & \boldsymbol{\rho}_n^+ \in \Delta S_n^+ \\ 0, & else \end{cases} \tag{8}$$

While the scatterer is divided into I triangular units, (6) can be expressed as

$$\mathbf{E}_S = \sum_{i=1}^{I} \left[\frac{\nabla}{4\pi\varepsilon j\omega} \int_{\Delta S_i} \nabla \cdot \mathbf{J}\left(\mathbf{r}'\right) \frac{e^{-jkR}}{R} dS - \frac{j\omega\mu}{4\pi} \int_{\Delta S_i} \mathbf{J}\left(\mathbf{r}'\right) \frac{e^{-jkR}}{R} dS \right] \tag{9}$$

Substituting (7) and (8) into (9), we have

$$\mathbf{E}_S = \sum_{i=1}^{I} \frac{J_n}{h_n^{\pm}} \left(\underbrace{\frac{\nabla}{4\pi\varepsilon j\omega} \int_{\Delta S_i} \pm 2 \cdot \frac{e^{-jkR}}{R} dS}_{\Phi_n} - \underbrace{\frac{j\omega\mu}{4\pi} \int_{\Delta S_i} \pm \boldsymbol{\rho}_n^{\pm} \frac{e^{-jkR}}{R} dS}_{\mathbf{A}_n} \right) \tag{10}$$

Choosing weight function $\mathbf{g}_m = \mathbf{f}_m$, the inner product between weight function and $\mathbf{E}_S$ is written as

$$\left\langle \mathbf{g}_m^{\pm}, \mathbf{E}_S \right\rangle = \sum_{i=1}^{I} J_n \left\langle -\nabla \cdot \mathbf{g}_m^{\pm}, \frac{1}{4\pi\varepsilon j\omega} \int_{\Delta S_i^{\pm}} \frac{\pm 2}{h_n^{\pm}} \cdot \frac{e^{-jkR}}{R} dS \right\rangle + \sum_{i=1}^{I} J_n \left\langle \mathbf{g}_m^{\pm}, -\frac{j\omega\mu}{4\pi} \int_{\Delta S_i^{\pm}} \frac{\pm \boldsymbol{\rho}_n^{\pm}}{h_n^{\pm}} \frac{e^{-jkR}}{R} dS \right\rangle \tag{11}$$

From (11), the impedance matrix Z_{mn} associated with edges m and n can be written as

$$Z_{mn} = \Phi_{mn} + A_{mn} \tag{12}$$

where scalar potential matrix Φ_{mn} and vector magnetic potential matrix A_{mn} are expressed as follows

$$\Phi_{mn} = -\left\langle \nabla \cdot \mathbf{g}_m^{\pm}, \Phi_n \right\rangle \tag{13}$$

and

$$A_{mn} = \left\langle \mathbf{g}_m^{\pm}, \mathbf{A}_n \right\rangle \tag{14}$$

The final expression of the matrix equation is

$$[Z_{mn}][J_n] = [V_m] \tag{15}$$

TABLE 2. Comparison of calculated and measured results.

Frequency (MHz)		2.56	3.27	3.39	4.1	4.24	4.49
measurement (dBμV/m)	0	25.8	35.1	34.1	25.5	24.4	28.3
	1/4λ	40.3	40.5	38.2	41.3	43.0	44.4
	1/2λ	24.2	27.1	30.8	32.0	29.6	29.9
	3/4λ	28.8	29.5	26.6	35.3	35.8	40.1
	λ	31.1	28.3	31.1	31.4	28.2	30.0
calculation (dBμV/m)	0	31.3	29.5	30.0	39.9	40.7	33.7
	1/4λ	32.4	36.3	32.3	38.5	40.4	38.8
	1/2λ	26.7	35.5	35.5	35.1	35.2	30.8
	3/4λ	30.3	28.6	31.8	38.9	40.6	38.1
	λ	33.5	37.5	31.5	37.1	36.0	30.4
difference (dB)	0	5.5	-5.6	-4.1	14.4	16.3	5.4
	1/4λ	-7.9	-4.2	-5.9	-2.8	-2.6	-5.6
	1/2λ	2.5	8.4	4.7	3.1	5.6	0.9
	3/4λ	1.5	-0.9	5.2	3.6	4.8	-2.0
	λ	2.4	9.2	0.4	5.7	7.8	0.4

TABLE 3. Parameters of MS2724C spectrum analyzer.

Parameter	Description
frequency	0.7 MHz - 3 MHz, 150 kHz - 30 MHz
detector	PK
bandwidth	10 kHz
measurement mode	sweep
trace	Maxhold

TABLE 4. Parameters of EMI receiver.

Parameter	Description
frequency	0.7 MHz - 3 MHz, 150 kHz - 30 MHz
detector	PK, QP
bandwidth	9 kHz
measurement mode	sweep, scan
trace	Maxhold, Clearwire

where V, the scatterer potential distribution, can be obtained from the measured voltage. Substituting $\mathbf{J}$ solving from (15) into (9), the electric fields can be calculated.

C. COMPARISON OF CALCULATED AND MEASURED RESULTS

Based on the aforementioned testing conditions, the simulation model of PLC is established using MOM. The model and testing electric field intensity at several typical frequency points are compared in Table 2. Data reveal that the calculated results are in good agreement with the measured results, and eighty percent (ninety percent) of differences are within 6 dB (9 dB). Although there are very few data with large differences, the accuracy of the model for predicting the distribution of PLC radiation in the field still meets the requirements in industrial applications.

III. FIELD MEASUREMENTS AND ANALYSIS

A. FIELD MEASUREMENTS

In China, power meter reading systems based on PLC are being promoted far and wide. At present, however,

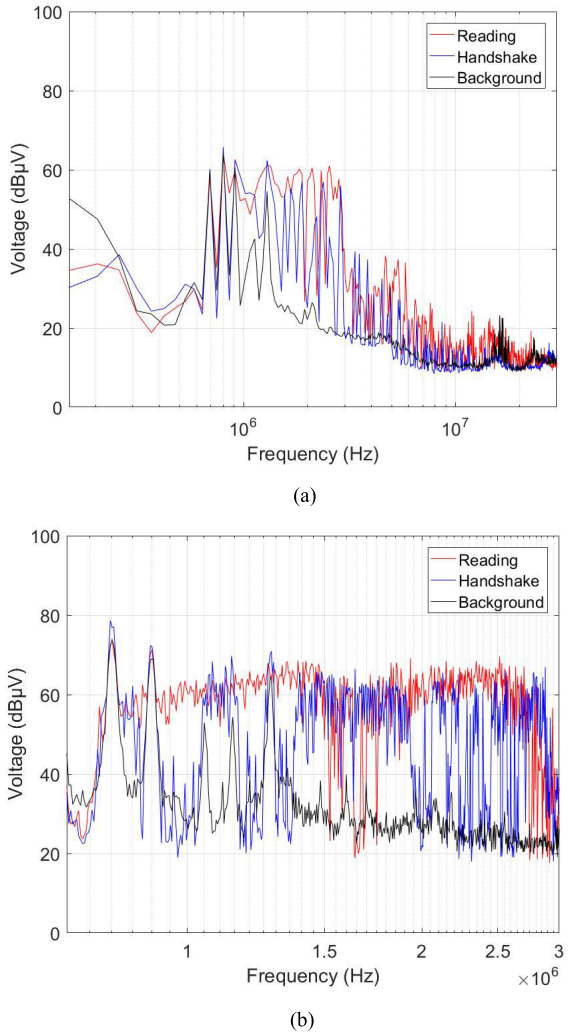

FIGURE 5. The A-to-N voltages at the beginning of the lines under three operating conditions. (a) 150 kHz – 30 MHz and (b) 0.7 MHz – 3 MHz.

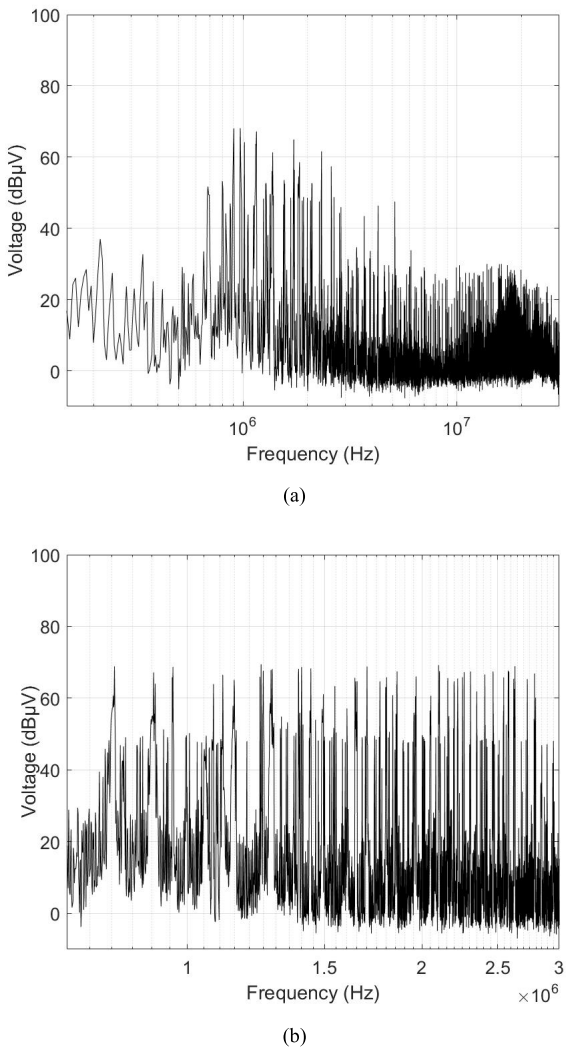

FIGURE 6. The A-to-N voltages at the beginning of the lines. (a) 150 kHz – 30 MHz and (b) 0.7 MHz – 3 MHz.

TABLE 5. Voltages at typical frequency points.

Frequency (MHz)	1.159	1.596	1.898	2.198	2.442	2.753
voltage (V)	0.1356	0.1089	0.1102	0.1539	0.1593	0.1486

TABLE 6. Electric field intensity in lateral direction.

Frequency (MHz)		1.159	1.596	1.898	2.198	2.442	2.753
electric fields (dBμV/m)	10 m	59.8	60.7	55.3	66.9	65.3	75.2
	30 m	49.1	50.4	49.0	54.4	47.7	54.5
	50 m	44.3	48.8	48.4	53.3	44.6	50.7
	70 m	50.2	47.2	46.4	49.1	47.1	47.8
	100 m	47.2	43.6	41.0	43.6	41.1	44.8
	150 m	45.4	41.2	40.5	40.4	40.3	42.3
	200 m	46.2	40.5	40.1	40.2	39.7	40.4

the electromagnetic radiation distribution characteristics at PLC application sites are insufficiently studied. There is no quantitative understanding of the radiated intensity from PLC systems. And it is inconclusive whether the existing guideline standards of PLC could be used as implementation standards.

Given all this, we choose several general practical application sites of power meter reading based on PLC, one EUT with 24 to 40 users in the working frequency range of 0.7-3 MHz, to carry out field research. The horizontal three-phase four-wire power lines are arranged above ground. The radius of each line is 4 mm. The spacing between four lines are 30 cm, 60cm, and 30 cm. And the heights of lines are 7.3-8.5 m in different sites. Because the sites are not open enough, it is impossible to carry out the measurement in full accordance with the recommended testing positions of FCC Part15. According to the characteristics of locations, we choose some positions that are close to the EUT, with few branch lines and relatively open. In order to compare the radiated intensity in different situations, three operating conditions of PLC system we set are: 1) handshake between the central coordinator (CCO) of EUT and the station (STA)

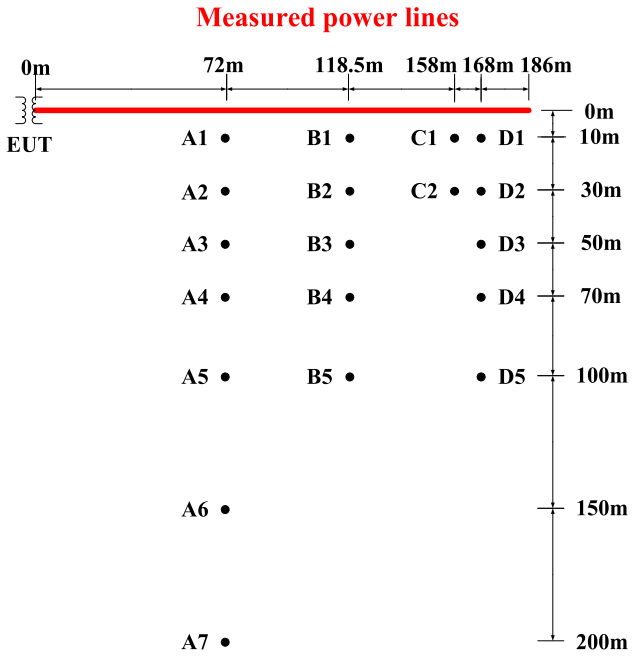

(a)

(b)

FIGURE 7. Field measurements for straight power lines. (a) Locations of measurement points and (b) scene photo.

of electric meter, 2) meter reading between CCO and STA and 3) without PLC (unplug CCO module). The voltage at the beginning of the power lines and the radiated intensity at typical measurement points in the area are measured under the three operating conditions. The parameter settings of the spectrum analyzer are shown in Table 3. The parameter settings of the EMI receiver are shown in Table 4.

1) MEASURED VOLTAGES

The A-to-N (A phase line to neutral line from power lines) voltages at the beginning of the lines under three operating conditions in the ranges of 150 kHz – 30 MHz and 0.7 MHz – 3 MHz are measured using the spectrum analyzer, as shown in Fig. 5. Note that the curves in Fig. 5 are based on Maxhold

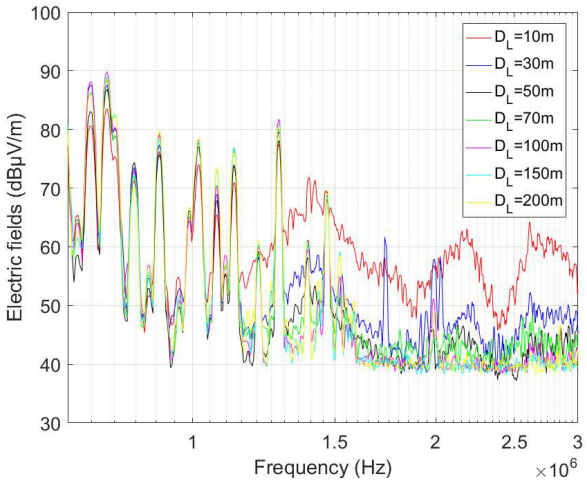

FIGURE 8. Radiated attenuation in lateral direction.

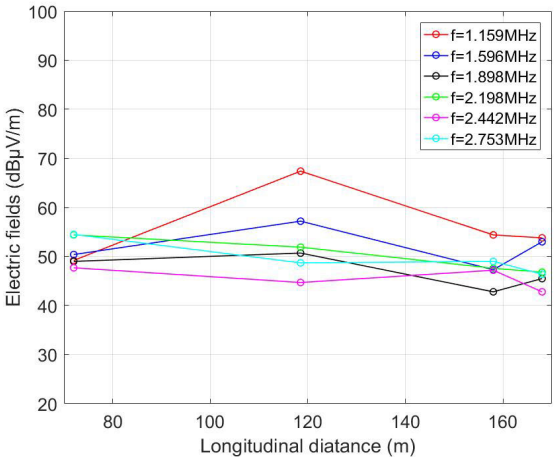

(a)

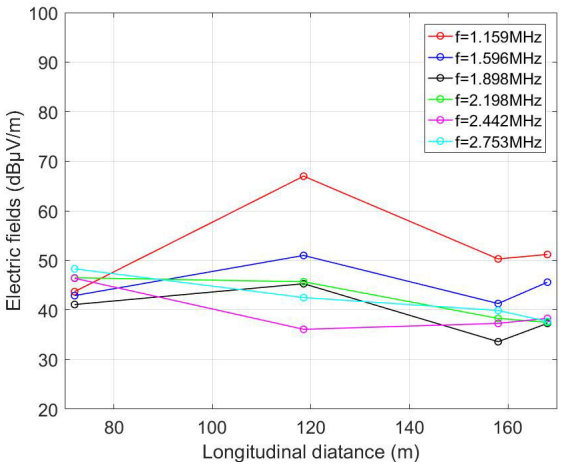

(b)

FIGURE 9. Longitudinal distribution of radiation. (a)Using a peak detector and (b) using a quasi-peak detector.

function, which means that these curves are not working waveforms of PLC. From Fig. 5, we can see that the voltages at the beginning of lines are obviously different under the

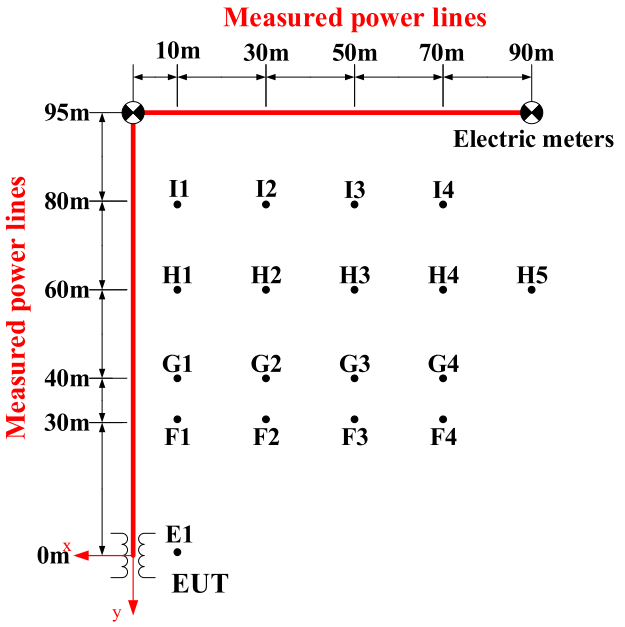

(a)

(b)

FIGURE 10. Field measurements for crossed power lines. (a) Locations of measurement points and (b) scene photo.

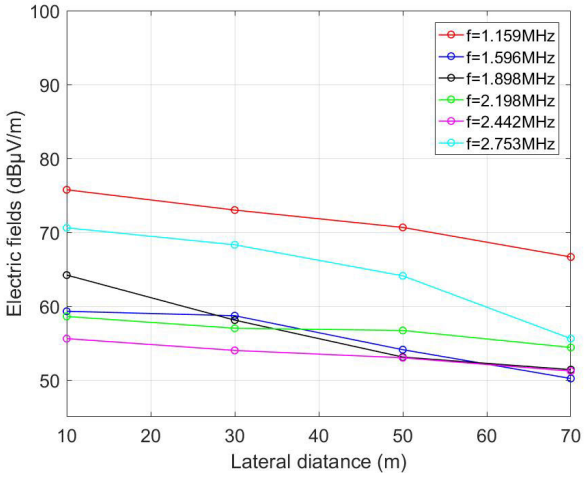

(a)

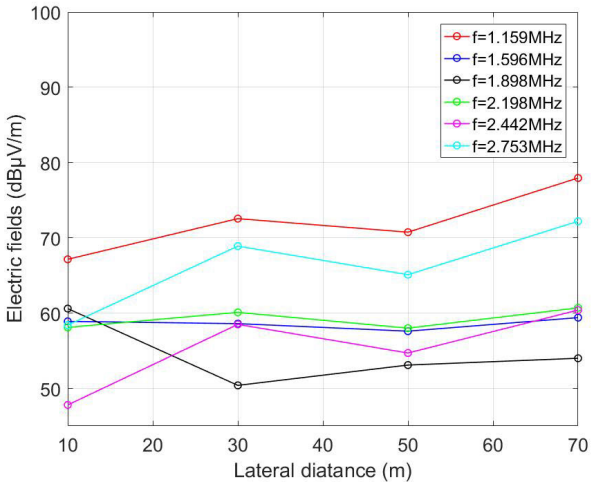

(b)

FIGURE 11. Radiated distribution of crossed power lines. (a) Measurement points F1 to F4 and (b) measurement points I1 to I4.

three operating conditions. The voltages under the condition of meter reading are generally larger than others, which can be inferred that the strongest radiated disturbance occurs in this situation. Therefore, what we measure in the rest of this paper is the radiation or voltage in this situation, unless otherwise specified. Figure 6 shows the A-to-N voltages measured at the beginning of the lines based on EMI receiver employing peak detector function and Clearwire measurement. The operating spectrum of PLC studied in this paper can be roughly predicted from Fig. 6.

Employing peak detector, scan measurement and Maxhold function of EMI receiver, a large number of measurements are performed to find several frequency points with large voltage in the working frequency range of 0.7-3 MHz, and 6 of them are selected as typical frequency points. In theory, the strongest radiation should also be generated at these frequency points, which is very representative for evaluating the severity of the electromagnetic environment. The voltages at typical frequency points are shown in Table 5.

2) RADIATED DISTRIBUTIONS OF STRAIGHT LINES

The radiated distributions of the straight power lines in the longitudinal direction (along the power lines) and the lateral direction (perpendicular to power lines) are measured. The locations of measurement points are illustrated in Fig. 7(a). The photo taken during the field measurement is shown in Fig. 7(b).

Using the spectrum analyzer, we obtain the radiated intensity attenuation of PLC within lateral measurement distances of 10-200 m (A1 to A7 in Fig. 7(a)), as shown in Fig. 8. It can be seen from Fig. 8 that the fluctuation of radiated intensity between the lateral measurement distances of 100 m, 150 m

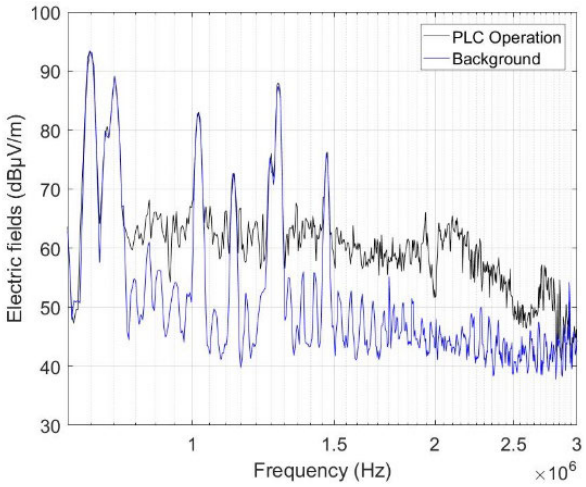

FIGURE 12. Comparison of radiated intensity of PLC operation and background noise.

and 200 m is small, which can be considered that the radiated intensity approaches to the background noise. Based on this, it can be estimated that when the PLC systems studied in this paper are working, the lateral operating range of radiated disturbance generated by straight power lines can be up to 100 m, or 150 m conservatively.

Employing peak detector, sweep measurement and Max-hold function of EMI receiver, we present in Table 6 the electric field intensity at typical frequency points when D_L = 10 m, 30 m, 50 m, 70 m, 100 m, 150 m and 200 m. Excluding individual data affected by the environment, the radiated disturbance intensity generally decreases with increasing lateral distance.

In the longitudinal direction (A2, B2, C2, and D2 in Fig. 7(a)), the measured radiation at typical frequency points using the peak detector and quasi-peak detector is shown in Fig. 9 (a) and Fig. 9 (b), respectively. We can see that the longitudinal distribution of radiation is fluctuant when PLC system is working. The reasons are: 1) affected by the standing wave characteristics and 2) affected by the distribution of meter branches along lines.

3) RADIATED DISTRIBUTIONS OF CROSSED LINES

We choose a more complicated application site, and measure the radiated distribution in the area where two perpendicular power lines intersect with each other. The locations of measurement points are illustrated in Fig. 10(a). The photo taken during the field measurement is shown in Fig. 10(b).

Figure 11(a) and 11(b) respectively show the radiated distribution trend at measurement points F1 to F4 and I1 to I4 employing peak detector, sweep measurement and Max-hold function of EMI receiver. Statistically speaking, the radiated intensity at these typical frequency points is generally large, and the data is representative, so these points are shown and compared with simulation. Since the measurement points F1 to F4 are located at the edge of the area, the radiated

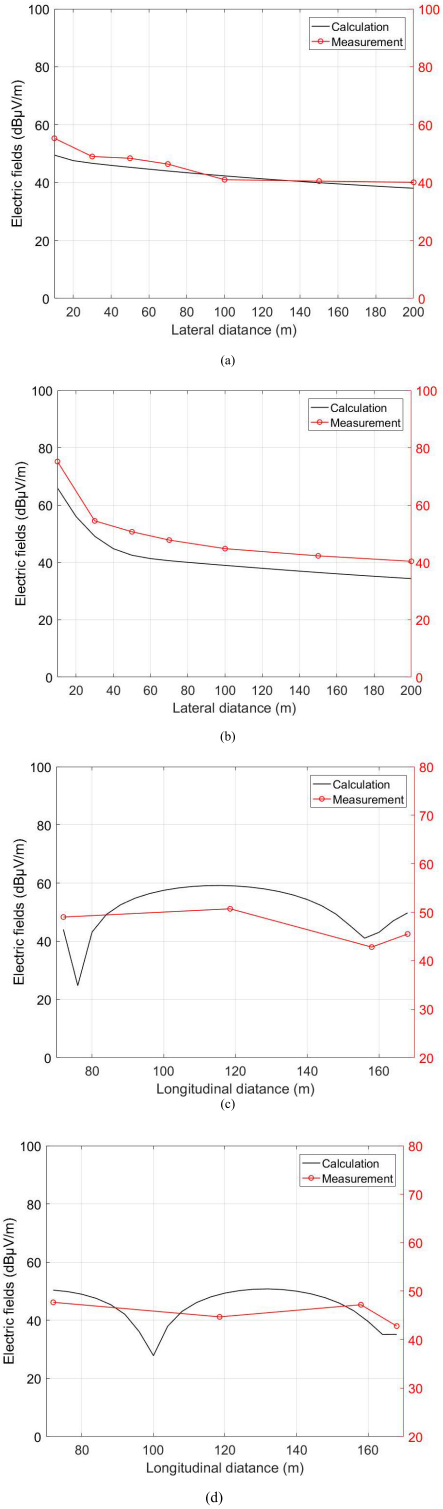

FIGURE 13. Comparison of calculated and measured results for straight lines. (a) Points A1 to A7 with 1.898 MHz. (b) Points A1 to A7 with 2.442 MHz. (c) Points A2, B2, C2, and D2 with 1.898 MHz. (d) Points A2, B2, C2, and D2 with 2.442 MHz.

distribution can also show a decreasing trend with increasing lateral distance. Just the radiated attenuation rate slows down due to the influence of crossed lines. However, the measurement points I1 to I4 are close to both power lines,

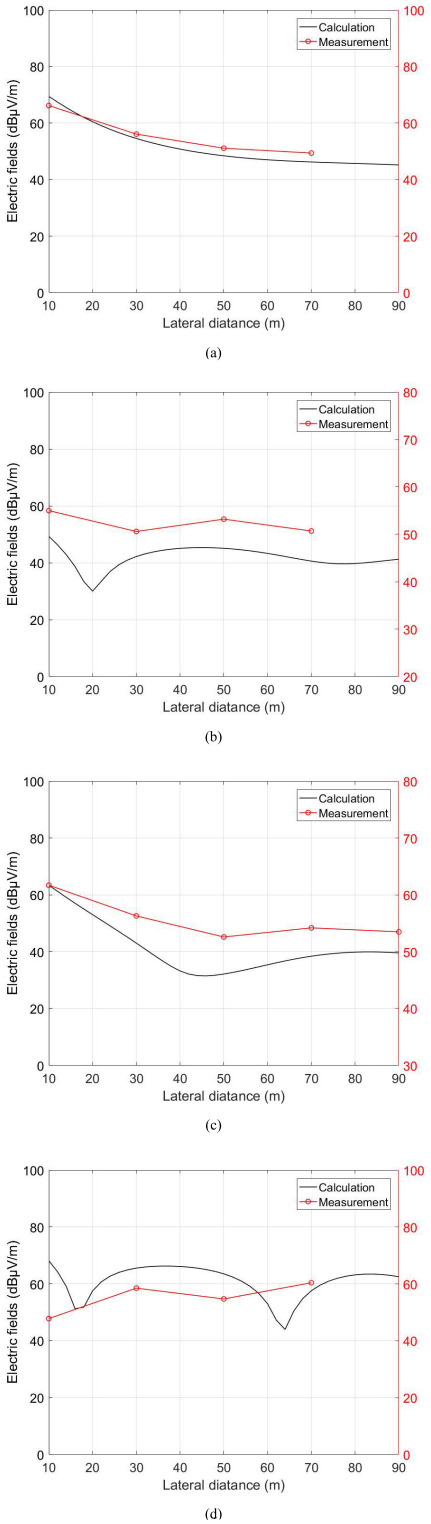

FIGURE 14. Comparison of calculated and measured results for straight lines. (a) Points F1 to F4 with 1.898 MHz. (b) Points G1 to G4 with 2.442 MHz. (c) Points H1 to H5 with 2.198 MHz. (d) Points I1 to I4 with 2.442 MHz.

the radiated distribution no longer has a trend of lateral attenuation like straight power lines, showing fluctuation and complexity.

4) ELIMINATE LOW-FREQUENCY ENVIRONMENTAL INTERFERENCE AND OBTAIN RADIATION CONTRIBUTION

From the former measurements, it is found that the radiated intensity is always large regardless of the lateral attenuation or longitudinal distribution at certain frequency points within 0.7-1.5 MHz, and hardly changes with the measurement locations. Therefore, we choose a suitable measurement point position with a lateral distance of 10 m, and obtain the radiated intensity of PLC and background noise in 0.7-3 MHz, as shown in Fig. 12. The results show that the electric field intensity significantly fall after the PLC system is turned off, but there are still some frequency points with large electric field intensity in 0.7-1.5 MHz, which proves that there are strong low-frequency interference sources, not PLC system, in the environment. The data of these interference sources should be excluded when studying the radiated distribution characteristics of PLC systems. It is clear from Fig. 12 that the electric field intensity when PLC operation is about 15 dB greater than the background noise at a lateral distance of 10 m. We define it as the radiated contribution value of field PLC system studied in this paper.

B. RECOMMENDATIONS FOR MEASUREMENT METHODS

In our analysis, there is a one-to-one correspondence between the maximum radiation and the maximum voltage during a sufficiently long measurement time, which is why we insist on using the Maxhold function. In addition, the maximum radiation, rather than transient radiation, is representative for evaluating the severity of the electromagnetic environment of PLC systems.

In terms of field measurement methods, recommendations are: 1) the data measured at typical frequency points shall be based on measuring equipment employing a peak detector, or quasi-peak detector, and Maxhold function. 2) the data measured within the bands PLC working and 0.15-30 MHz shall be based on measuring equipment employing Maxhold function, or Clearwire function, and a peak detector. Contributions can be calculated by comparing the radiated levels when PLC system is operating and turned off. Note that after unplugging the CCO module of EUT (meaning without PLC), it takes at least 15 minutes for field PLC systems to completely stop communication. In order to accurately study the radiated distribution characteristics, the locations of measurement points shall be carefully chosen according to the environment of application sites (e.g., proper measurement orientation and distance). Moreover, due to the changes of users, the measurement time shall also be strictly controlled. For example, the time interval between two tests used for comparison should not be too long.

C. SIMULATION ANALYSIS

Using the same calculation method of PLC radiation as before, simulation models for straight lines and crossed lines are established respectively. We present in Fig. 13 and Fig. 14 the trend comparison between calculated results and

measured data of electric field intensity. It is clear that radiated distribution trend is basically the same. Another observation one can notice is that, the measured data are generally larger than the calculation results. This is because the background noise induced by equipment, systems or environment other than measured power lines is already large, and cannot be considered in the simulation model. In terms of numerical relations, the measured data of PLC radiation are the vector sum of calculation results and background noise. Using the modeling method in this paper, the distribution trend of PLC radiation can be predicted to a certain extent. This is very useful for evaluating the radiated distribution characteristics of PLC in harsh electromagnetic environments.

IV. CONCLUSION

In this paper, we measure and analyze the electromagnetic radiation of the PLC system for power meter reading, which increases rapidly in China nowadays. The measured radiation data of PLC experimental system are basic anastomotic with the calculated results, which indicates that the simulation method based on MOM is effective. At application sites of PLC system, the strongest radiation and maximum voltage are obtained by analyzing the measured data under three operating conditions. For the straight power lines with one EUT and 24-40 users studied in this paper, longitudinal distribution of radiation is fluctuant, lateral attenuation rate of radiation is rapid. The radiated contribution value is about 15 dB at a lateral distance of 10 m. And the radiated intensity is close to the background noise at a lateral distance of 100 m (or 150 m conservatively). For the area where crossed power lines work together, the radiated distribution with nonuniformity of PLC is clarified. With the simulation model, the radiated distribution characteristics of the PLC system can be predicted. In addition, some recommendations for measurement methods are proposed.

REFERENCES

[1] S. Galli, A. Scaglione, and Z. Wang, "For the grid and through the grid: The role of power line communications in the smart grid," *Proc. IEEE*, vol. 99, no. 6, pp. 998–1027, Jun. 2011, doi: 10.1109/JPROC.2011.2109670.

[2] C. Cano, A. Pittolo, D. Malone, L. Lampe, A. M. Tonello, and A. G. Dabak, "State of the art in power line communications: From the applications to the medium," *IEEE J. Sel. Areas Commun.*, vol. 34, no. 7, pp. 1935–1952, Jul. 2016, doi: 10.1109/JSAC.2016.2566018.

[3] A. Ikpehai, B. Adebisi, K. Rabie, R. Haggar, and M. Baker, "Experimental study of 6LoPLC for home energy management systems," *Energies*, vol. 9, no. 12, p. 1046, Dec. 2016.

[4] M. Zimmermann and K. Dostert, "A multipath model for the powerline channel," *IEEE Trans. Commun.*, vol. 50, no. 4, pp. 553–559, Apr. 2002, doi: 10.1109/26.996069.

[5] B. Adebisi, J. Stott, and B. Honary, "Experimental study of the interference caused by PLC transmission on HF bands," in *Proc. 10th IET Int. Conf. Ionospheric Radio Syst. Techn. (IRST)*, Beijing, China, Jul. 2006, pp. 326–330.

[6] E. S. Hassan, "Multi user MIMO-OFDM-based power line communication structure with hardware impairments and crosstalk," *IET Commun.*, vol. 11, no. 9, pp. 1466–1476, Jun. 2017, doi: 10.1049/iet-com.2016.0952.

[7] L. Lampe and A. J. H. Vinck, "Cooperative multihop power line communications," in *Proc. IEEE Int. Symp. Power Line Commun. Appl.*, Beijing, China, Mar. 2012, pp. 1–6.

[8] B. Nikfar and A. J. H. Vinck, "Relay selection in cooperative power line communication: A multi-armed bandit approach," *J. Commun. Netw.*, vol. 19, no. 1, pp. 1–9, Feb. 2017, doi: 10.1109/JCN.2017.000003.

[9] W. Bakkali, P. Pagani, and T. Chonavel, "Energy efficiency performance of relay-assisted power-line communication networks," in *Proc. 12th Annu. IEEE Consum. Commun. Netw. Conf. (CCNC)*, Las Vegas, NV, USA, Jan. 2015, pp. 525–530.

[10] W. Bakkali, P. Pagani, T. Chonavel, and A. M. Tonello, "Energy efficiency performance of decode and forward MIMO relay PLC systems," in *Proc. Int. Symp. Power Line Commun. Appl. (ISPLC)*, Bottrop, Germany, Mar. 2016, pp. 201–205.

[11] K. M. Rabie, B. Adebisi, H. Gacanin, and S. Yarkan, "Energy-per-bit performance analysis of relay-assisted power line communication systems," *IEEE Trans. Green Commun. Netw.*, vol. 2, no. 2, pp. 360–368, Jun. 2018, doi: 10.1109/TGCN.2018.2794613.

[12] M. Rozman, A. Ikpehai, B. Adebisi, and K. M. Rabie, "Channel characterisation of cooperative relaying power line communication systems," in *Proc. 10th Int. Symp. Commun. Syst., Netw. Digit. Signal Process. (CSNDSP)*, Prague, Czech Republic, Jul. 2016, pp. 1–5.

[13] F. Canete, J. Cortes, L. Diez, and J. Entrambasaguas, "A channel model proposal for indoor power line communications," *IEEE Commun. Mag.*, vol. 49, no. 12, pp. 166–174, Dec. 2011, doi: 10.1109/MCOM.2011.6094022.

[14] H. Liu, J. Song, B. Zhao, and X. Li, "Channel study for medium-voltage power network," in *Proc. IEEE Int. Symp. Power Line Commun. Appl.*, Orlando, FL, USA, Mar. 2006, pp. 245–250.

[15] A. Oka and L. Lampe, "Compressed sensing reception of bursty UWB impulse radio is robust to narrow-band interference," in *Proc. IEEE Global Telecommun. Conf. (GLOBECOM)*, Honolulu, HI, USA, Nov. 2009, pp. 1–7, doi: 10.1109/GLOCOM.2009.5425245.

[16] A. Gomaa and N. Al-Dhahir, "A sparsity-aware approach for NBI estimation in MIMO-OFDM," *IEEE Trans. Wireless Commun.*, vol. 10, no. 6, pp. 1854–1862, Jun. 2011, doi: 10.1109/TWC.2011.040411.101118.

[17] K. A. Saaifan and W. Henkel, "A receiver design for MIMO systems over Rayleigh fading channels with correlated impulse noise," in *Proc. IEEE Global Commun. Conf. (GLOBECOM)*, Anaheim, CA, USA, Dec. 2012, pp. 2481–2486, doi: 10.1109/GLOCOM.2012.6503489.

[18] J. D. Kraus, *Antennas for All Applications*, 3rd ed. New York, NY, USA: McGraw-Hill, 2001.

[19] S. Battermann and H. Garbe, "Influence of PLC transmission on the sensitivity of a short-wave receiving station," in *Proc. Int. Symp. Power Line Commun. Appl.*, Vancouver, BC, Canada, 2005, pp. 224–227, doi: 10.1109/ISPLC.2005.1430501.

[20] *Electronic Code of Federal Regulations, FCC Part 15*, Radio Freq. Devices, Federal Commun. Commission, Washington, DC, USA, 2019.

[21] S. Rao, D. Wilton, and A. Glisson, "Electromagnetic scattering by surfaces of arbitrary shape," *IEEE Trans. Antennas Propag.*, vol. AP-30, no. 3, pp. 409–418, May 1982, doi: 10.1109/TAP.1982.1142818.

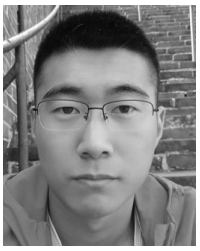

WENJUN PENG was born in Anqing, China, in 1995. He is currently pursuing the M.Sc. degree in electrical engineering with North China Electric Power University, Beijing, China.

His main research interests are electromagnetic environments and electromagnetic compatibility in electric power systems.

WEIDONG ZHANG was born in Baoding, China, in 1967. He received the B.Sc. degree in electromagnetic field and microwave technology from the Beijing Broadcasting Institute, Beijing, China, in 1990, and the M.Sc. and Ph.D. degrees in electrical engineering from the North China Electric Power University, Baoding, in 1996 and 2003, respectively.

He is currently a Professor with the School of Electrical and Electronic Engineering, North China Electric Power University. His research areas include electromagnetic environments, electromagnetic compatibility in electric power systems, and transient measurement techniques in various applications.

BO AN was born in Baoding, China, in 1978. He received the B.Sc. degree in electrical engineering from North China Electric Power University, Baoding, in 2001, the M.Sc. degree in electronic engineering from the Delft University of Technology, The Netherlands, in 2003, and the Ph.D. degree in electrical engineering from North China Electric Power University, in 2017.

He is currently a Lecturer with the School of Electrical Engineering, North China Electric Power University. His research areas include electromagnetic environments, electromagnetic compatibility in electric power systems, and transient measurement techniques in various applications.